International Journal of Neural Systems

Preprint of an article published in International Journal of Neural Systems, 28(1), 2018, 1750032
10.1142/S0129065717500320 *© copyright World Scientific Publishing Company*
https://www.worldscientific.com/worldscinet/ijns

QUANTIFICATION OF GRAPH COMPLEXITY BASED ON THE EDGE WEIGHT DISTRIBUTION BALANCE: APPLICATION TO BRAIN NETWORKS

JAVIER GOMEZ-PILAR[1], JESÚS POZA*[1,2,3], ALEJANDRO BACHILLER[1], CARLOS GÓMEZ[1], PABLO NÚÑEZ[1], ALBA LUBEIRO[4], VICENTE MOLINA[3,4,5], ROBERTO HORNERO[1,2,3]

[1]*Biomedical Engineering Group, E.T.S. Ingenieros de Telecomunicación, Universidad de Valladolid, Paseo Belén, 15, 47011 Valladolid, Spain*
[*]jesus.poza@tel.uva.es

[2]*IMUVA, Instituto de Investigación en Matemáticas, Universidad de Valladolid, Valladolid, Spain*

[3]*INCYL, Instituto de Neurociencias de Castilla y León, Universidad de Salamanca, Salamanca, Spain*

[4]*Psychiatry Department, Facultad de Medicina, Universidad de Valladolid, Valladolid, Spain*

[5]*Clinical University Hospital of Valladolid, Valladolid, Spain*

The aim of this study was to introduce a novel global measure of graph complexity: Shannon Graph Complexity (*SGC*). This measure was specifically developed for weighted graphs, but it can also be applied to binary graphs. The proposed complexity measure was designed to capture the interplay between two properties of a system: the 'information' (calculated by means of Shannon entropy) and the 'order' of the system (estimated by means of a disequilibrium measure). *SGC* is based on the concept that complex graphs should maintain an equilibrium between the aforementioned two properties, which can be measured by means of the edge weight distribution. In this study, *SGC* was assessed using four synthetic graph datasets and a real dataset, formed by electroencephalographic (EEG) recordings from controls and schizophrenia patients. *SGC* was compared with graph density (*GD*), a classical measure used to evaluate graph complexity. Our results showed that *SGC* is invariant with respect to *GD* and independent of node degree distribution. Furthermore, its variation with graph size (N) is close to zero for $N > 30$. Results from the real dataset showed an increment in the weight distribution balance during the cognitive processing for both controls and schizophrenia patients, though these changes are more relevant for controls. Our findings revealed that *SGC* does not need a comparison with null hypothesis networks constructed by a surrogate process. In addition, *SGC* results on the real dataset suggest that schizophrenia is associated with a deficit in the brain dynamic reorganization related to secondary pathways of the brain network.

Keywords: Graph theory, brain networks, brain complexity, entropy.

1. Introduction

The application of graph-theoretical analyses to study brain networks constitutes an evolving field with a high impact in neuroscience. The characterization of brain networks in terms of integration, segregation, regularity or complexity has become of paramount importance to identify the underlying processes of the functional neural organization in the brain. In order to understand brain network behavior, previous works conducted resting-state activity analyses[1,2] as well as task-related activity ones.[3–5] Both together provide an overall view of brain networks generated under different conditions. Functional complex brain networks are usually depicted by a set of nodes (vertices) and connections (edges or links). These connections represent the statistical

dependence between neural activity in different brain areas, obtained by correlations, mutual information or coherence, among others.[6,7] Most brain graph studies use binary connections between nodes (i.e., a threshold is applied to dichotomize the edge weights.[8] Although this is an apparently simple model, these graph analyses are interpretable in relation to general principles of complex system organization.[8] On the other hand, weighted network analysis introduces the concept of connection strength between nodes. It can be considered a more realistic approach of the physiological properties of brain networks.[8,9] Unfortunately, the use of weighted graphs is not exempt from methodological concerns, which have not been completely solved yet. [9]

A high amount of measures have been proposed to describe the organization and function of brain networks.[10–12] These network measures are usually defined for binary graphs and, when possible, generalized for more complex graphs, such as weighted and/or directed graphs. Roughly speaking, network measures can be divided into two classes depending on the nodes involved: (i) local measures, related to a single node or edge (for the computation other nodes/edges can be involved, even all of them), and (ii) global measures, which describe the properties of the entire network. Usually, global network measures are strongly influenced by basic properties, such as network size (N), graph density (GD) and node degree distribution.[9] For instance, consider a graph **A**, as a complete, binary and undirected graph with $N = 10$ nodes, and a graph **B** with equal basic characteristics (complete, binary and undirected), but with $N = 100$ nodes. Node degree distributions are similar for both cases, and the maximum GD possible for each respective N is reached for these two graphs. Although both graphs have similar topology and their main difference is N, the characteristic path length (i.e., the average shortest path length between all pairs of nodes in the network[13]) of graph **A** is much lower than that of the graph **B** because of the network size. Consequently, the statistical significance of the network parameters must be considered by comparing them with null-hypothesis networks (i.e., networks constructed by surrogate process).[11] Null-hypothesis networks can be modeled as networks with the same basic characteristics as the original network (N, GD and node degree distribution), but with different topology.[11] Null models are often used as a reference point to determine whether a graph displays a topological feature to a greater extent than expected by chance. To date, the most widespread method to construct null-hypothesis weighted networks is based on applying a random rewiring process.[1] Although there are several ways to generate these null-hypothesis networks, none of them are bias-free for weighted graphs.[9] There are even graph methodologies that remove non-relevant connections from the brain graphs by means of techniques based on the percentile[14] or the p-value[15], making surrogate processes completely necessary, even when the same electrode configuration is used.

It is generally accepted that the brain is a well-designed anatomical network, which exhibits an optimal balance between functional integration and segregation.[6,16] On the other hand, pathological networks are usually accompanied by diverse alterations and/or deficits in network functions. However, contradictory results have been found after computing measures of integration or segregation when some specific diseases were studied. Discrepancies in brain network properties can occur due to several reasons: the method of edge weight assignment, the thresholding method used to construct binary graphs (when these are considered instead of weighted graphs) or the surrogate process used to compare with null-hypothesis networks, among others. Nevertheless, there is consensus about the high complexity of the brain when compared to other networks, such as regular or random configurations.[17] Although the study of complex networks has provided us with a further understanding of brain coupling dynamics,[18–21] the underlying concern is that there is not a widely accepted scientific definition of graph complexity. Several complexity measures have attempted to capture the intuitive notion of complexity by emphasizing the idea that complex systems are neither completely regular nor completely random.[22] In this context, a number of graph complexity measures have been proposed to assess brain behavior. This is the case of the study of Ahmadlou *et al.*,[23] which proposed the power of scale-freeness of a graph structure and the maximum eigenvalue of the adjacency matrix of a graph as features to measure graph complexity. For that purpose, they used Visibility Graph Similarity (VGS) a recently introduced concept to accurately quantify the overall synchronization in both identical and non-identical couplings of time series.[24] Machta and Machta[25] proposed the computational complexity of a parallel algorithm, to evaluate brain behavior. Meyer-Ortmanns[26]

associated the complexity of the network with the number of topologically non-equivalent graphs generated by selecting vertices and partitioning the edges of the original vertex among the new vertices. There are even measures that define graph complexity in the context of information theory.[22,27,28] Tononi *et al.*[22] reported an elaborate new concept of complexity based on mutual information, which relies on the coexistence of functional specialization and integration. Morabito *et al.*[28] used mutual information to construct the connectivity matrix. Claussen[27] defined off-diagonal complexity, computed by the entropy of a vertex-vertex edge correlation matrix. Nonetheless, all these measures are influenced by network topology, making surrogate processes necessary. This implies an additional source of possible confusion that it is convenient to avoid. To date, none of them have been generalized for weighted graphs. In our opinion, the weighted graph model is more appropriate than the binary one to analyze brain dynamics, since it provides a realistic framework to address the characterization of the neural substrates of the brain. Thus, a new and complementary graph complexity measure, not influenced by network topology, is pertinent.

The main objective of this study was to introduce Shannon Graph Complexity (*SGC)*, a novel graph measure based on the assumption that a complex network is a system that can be modeled as a graph that should maintain equilibrium between the 'order' and the amount of 'information' stored. *SGC* should meet three requirements: (i) it should be able to measure the aforementioned interplay, (ii) it should be independent of the network topology, and (iii) it should not require a comparison with null-hypothesis networks. Our primary hypothesis for the mathematical definition of *SGC* states that, for a fixed topology, the weight distribution of a complex network is directly related to its reliability and information propagation speed. The second objective of the present study was to assess the usefulness of *SGC* in determining the properties of the real brain networks. Specifically, real graphs were obtained from the electroencephalographic (EEG) signals of controls and schizophrenia patients during an auditory oddball task. In this regard, we hypothesize that pathological neural substrates affecting network connectivity[29] can be characterized by analyzing the balance of the weight distribution by means of *SGC*.

This paper is divided into six sections. In Section 2, the theoretical ground of *SGC* is introduced. Section 3 describes the four synthetic and the real EEG datasets used in the study. The simulation results for synthetic data and the results obtained from EEG recordings are shown in Section 4. Finally, we discuss the implications of these results and summarize the main conclusions of the study.

2. Complex network measures

2.1. *Null-hypothesis models and traditional global measures*

Several null-hypothesis networks have been proposed to accurately assess brain graphs. The two most used weighted null-hypothesis networks are: (i) null-hypothesis networks that preserve *N*, *GD* and edge weight distribution by means of a connection reshuffling process[1]; and (ii) null-hypothesis networks that preserve *N*, *GD* and the degree of each node.[30] It is important to note that none of the two null-hypothesis networks preserve node degree distribution for weighted graphs, especially if the weight distribution is nonhomogeneous.[11] Ansmann *et al.*[9] compared these two kinds of surrogate processes and the non-surrogate model. They concluded that weight-preserving null-hypothesis networks could segregate the influence of basic parameters more accurately than degree-preserving network model and the model performed without any surrogate process. However, all the previous methods are not bias-free.[9] Even though the bias is always present in any measure, the bias introduced via surrogate data must be reduced as much as possible for preventing inappropriate conclusions.[9] Specifically, this bias could be the reason of the previously mentioned contradictory results in graph measures when some specific diseases were studied. To overcome this issue, three options can be proposed. The first one is to accept the bias introduced by the weight-preserving surrogate process; nonetheless, this additional source of bias could yield contradictory results. The second option is to design a new non-biased method, though some researches claim that an "unbiased method for empirical data does not exist".[31] Due to the drawbacks of the previously mentioned options, we chose the third one: to define a global graph measure that does not need a surrogate process.

Indeed, there are network measures, such as *GD*, that do not need a surrogate process, when comparing

networks with the same *N*. *GD* values are identical in the original network and in the null-hypothesis networks constructed using the weight-preserving approach. Thereby, this measure does not depend on the node degree distribution and normalization is not required. *GD* is then an appropriate measure to validate *SGC*, not only because a surrogate process is not needed to compute both measures, but also because *GD* can be used to estimate network complexity.[10,12] In fact, Bonchev and Buck renamed *GD* for binary graphs as 'normalized edge complexity'.[12] In addition, *GD* indicates the connectivity of the network, since it provides a measure of the average weight of the graph edges. For undirected, weighted networks without self-loops, *GD* can be mathematically defined as follows:

$$GD = \frac{\sum_{i=1}^{N}\sum_{j>i} w_{ij}}{T}, \quad (1)$$

where w_{ij} represents the edge weight between nodes *i* and *j*, and $T = N(N-1)/2$ is the total number of connections in a undirected graph.

2.2. *Shannon Graph Complexity*

Most of the complexity definitions proposed in previous studies have different drawbacks: (i) high computational cost; (ii) difficulty to be generalized for weighted graphs; and (iii) influence of network topology. This influence is not a problem by itself but, to segregate the influence of the topology, a comparison with null-hypothesis networks becomes necessary, especially for small networks typically derived from the study of functional connectivity using EEG signals.[9] In order to overcome these limitations, we introduce a novel definition of complexity that is independent of network topology. In our preliminary study,[32] we defined a novel graph complexity measure based on information theory, nevertheless, the dependences on basic network parameters were not assessed. *SGC* is based on analyzing the weight distribution balance of the network. This statistical complexity measure considers that the weight distribution of a graph can be measured in terms of 'order' and 'information'. To capture this interplay, *SGC* was defined as the product of the Shannon graph entropy (*H*) and the statistical disequilibrium (*D*):

$$SGC = H \cdot D. \quad (2)$$

Firstly, for the computation of *H*, we rely on the definition of Shannon entropy,[33] as a measure of the stochastic edge weight distribution. *H* is given by the following formula[12]:

$$H = \frac{-1}{\log_2 T}\sum_{i=1}^{N}\sum_{j>i}\frac{w_{ij}}{W}\log_2\frac{w_{ij}}{W}, \quad (3)$$

where *W* is the sum of all weights of the graph and $\log_2 T$ is a normalization factor introduced to ensure that $0 \leq H \leq 1$.

Secondly, *D* is defined as the statistical distance in the probability space between the equilibrium distribution and the weighted distribution of the graph under study.[34] It is noteworthy that the distribution with uniform weights (i.e., weights with the same value) is considered as the equilibrium distribution in Gibbs' statistical mechanics.[34] Thereby, a highly balanced weighted graph (such as a graph with all weights equally valued) yields a maximum Shannon graph entropy, $H^{\text{balanced}} = 1$, and a value of *D* equal to zero. On the contrary, a highly unbalanced weighted graph distribution gives $H^{\text{unbalanced}} \approx 0$ and a high *D* value. In this study, the Euclidean distance was used to compute *D* as follows:

$$D = \sqrt{\frac{1}{T-1}} \cdot \frac{\sigma}{\bar{w}}. \quad (4)$$

where $\bar{w}$ is the average of all edge values of the graph and σ is the standard deviation of those values.
In equation (4), *D* was normalized to take values in the 0-1 interval, dividing by its maximum value.[34]

In a different context, this concept of complexity was defined by López-Ruiz *et al.*[35] The authors defined a statistical measure of complexity as a balance between 'order' and amount of 'information'. They proposed that a crystal might have maximum 'order' and minimum 'information' (the structure can be described using two or three parameters). Conversely, an ideal gas would have minimum 'order' and maximum 'information'. They are examples of simple models and, therefore, systems with zero complexity.[35] The parallelism between a lattice graph and the description of a crystal in terms of 'information' and 'order' is clear. On the other hand, an ideal gas can be seen as an unbalanced graph. Therefore, it is expected that these two kinds of graphs have complexity values close to zero.

It is noteworthy that, by definition, *SGC* depends on both *N* and the weight distribution balance, but it is normalized with respect to *GD* and is independent of node degree distribution. To illustrate these issues, four

synthetic datasets were generated by varying different network properties.

3. Simulated and real data

To perform the simulations of synthetic graphs and to analyze the real data, we used Matlab® R2013b (MathWorks Inc., USA) by means of custom scripts and the available functions on Statistics and Machine Learning Toolbox and Signal Processing Toolbox. In addition, EEGLAB toolbox was used to carry out the Independent Component Analysis (ICA) over the EEG data in order to remove artifacts.

3.1. *Synthetic graphs*

In this section, we describe four synthetic graph datasets. Synthetic graphs were generated by varying: (i) *N*; (ii) the unbalancing factor, *UF* (i.e., a measure of the unbalancing strength, which is defined as the number of times the largest graph edge value is greater than the lower one); (iii) *GD*; and (iv) the node degree distribution (i.e., distribution of the sum of the weights reaching to each node). The datasets were constructed in order to study the *SGC* dependences on the previous variables in terms of weight balance. Fig. 1 illustrates the construction process for the four datasets.

DATASET-1: In order to determine the *SGC*-dependence on *N* and *UF*, DATASET-1 was generated as follows:

(i) Consider a weighted and undirected graph with size *N* in which all the edges, except one, have a fixed value of 1. The remaining edge was set to the *UF* value.

(ii) An edge with a value 1 was randomly chosen and replaced by the *UF* value, obtaining a new graph.

(iii) Step ii was repeated until all edges were set to the *UF* value. The last graph is defined as a completely balanced graph.

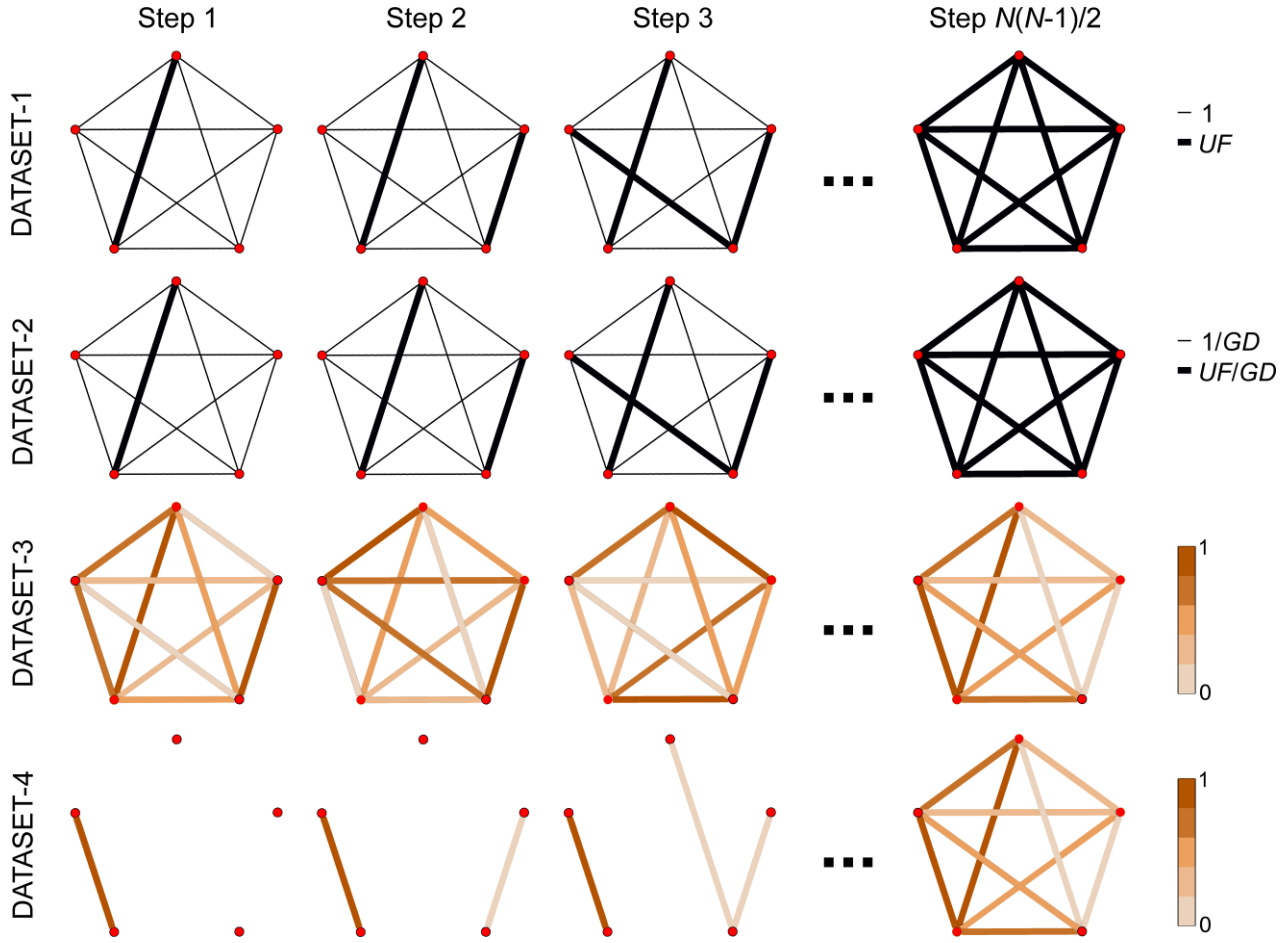

Fig. 1. Dataset construction examples for $N = 5$. Each row exemplifies the construction of one of the datasets.

(iv) The process was repeated for all combinations of network sizes with $N \in \{2, 3,\ldots, 128\}$ and different values of $UF \in \{2, 10, 10^2, 10^3, 10^4, 10^5\}$. The maximum value of N was selected for being the typical value of the number of electrodes in high density EEG recordings. On the other hand, *UF* was chosen in order to comprise a range of values large enough to accurately assess *SGC* dependences.

This dataset is comprised of $6\sum_{N=2}^{128} N(N-1)/2 =$ 2,097,024 adjacency matrices with sizes between 2×2 and 128×128, 6 different *UF* values and a single change in each of their connections (there are a total of $N(N-1)/2$ connections in each graph).

DATASET-2: This dataset was used to characterize the graph complexity when *N* and *UF* change, but *GD* remains constant. Construction of DATASET-2 is similar to the generation of DATASET-1, except that all graphs were normalized by their *GD*. Thus, edge weights in DATASET-2 were proportional to DATASET-1, but their *GD* was fixed to 1.

DATASET-3: The purpose of this dataset was to determine the dependence of *SGC* on the node degree distribution. The generation of DATASET-3 can be summarized as follows:

(i) Consider a weighted and undirected graph with fixed size (N = 31), where all the edges values are randomly distributed. The value of *N* was chosen in order to coincide with the number of EEG electrodes in the DATASET-real (see next subsection for details).
(ii) A new graph was constructed by randomly reshuffling the edge weights. By means of this process, different node degree distributions were obtained, but maintaining the same weight distribution.
(iii) Step ii was repeated 999 times, obtaining a total of 1000 graphs with the same weights, but different node degree distributions.
(iv) All the previous steps were performed for three different distributions of edge values: a uniform distribution from 0 to 1 edge values, a normal distribution (0.5 ± 0.1, mean ± standard deviation, SD) and a bimodal distribution constructed as the mixture of two normal distributions (1/3 ± 0.1 and 2/3 ± 0.1, mean ± SD).

It is important to note that we ensured that all edge values ranged from 0 to 1. Thus, 3000 (1000 of each type) graph formed this DATASET-3.

DATASET-4: The purpose of this dataset was to study the behavior of *SGC* for graphs with different number of connections. The DATASET-4 construction is summarized as follows:

(i) Consider an empty graph (edgeless graph) with size *N*.
(ii) An aleatory edge between two disconnected nodes was set to a random value from 0 to 1 (edge values were uniformly distributed between those values).
(iii) Step ii) was repeated until all edges were connected. The last graph is defined as a fully connected graph.
(iv) The process was repeated for all combinations of network sizes with $N \in \{2, 3,\ldots, 128\}$. As in the DATASET-1 and DATASET-2, the maximum value of N was selected for being a common value of the number of electrodes in high density EEG recordings.

This dataset is comprised of $\sum_{N=2}^{128} N(N-1)/2 =$ 349,504 adjacency matrices with sizes between 2×2 and 128×128.

3.2. *Real EEG data*

As an example of application on real graphs, a real dataset (DATASET-real hereinafter) was included in this study. Connectivity patterns come from the EEG recordings of 51 healthy controls and 28 schizophrenia patients. Diagnosis was made by and expert clinician involved in the treatment of the patients according to Diagnostic and Statistical Manual of Mental Disorders, 5th edition (DSM-V) criteria.[36] The clinical status of schizophrenia patients was scored using the Positive and Negative Syndrome Scale (PANSS).[37] Demographics and clinical characteristics of schizophrenia patients and controls are summarized in Table 1. In order to avoid medical conditions, which might influence the results, controls and schizophrenia patients were selected using inclusion/exclusion criteria based on clinical history and structured interviews (see Refs. 3 and 4 for a complete description). No significant between-group differences ($p > 0.05$) were found in age (Wilcoxon signed-rank test)

Table 1. Demographic and clinical characteristics. Values are shown as 'mean ± standard deviation (SD). NA means 'not applicable'. M: male. F: female.

Characteristic	SCH Patients	Controls
Age (years)	31.19 ± 10.43	29.31 ± 9.74
Gender (M:F)	13:15	24:27
PANSS–positive	11.39 ± 3.40	NA
PANSS–negative	18.26 ± 8.24	NA
PANSS–total	54.00 ± 21.47	NA

or gender (Chi-squared test). All participants gave their informed consent prior to their participation in the study. Moreover, the study protocol was approved by the local Ethics Committee of Clinical University Hospital of Valladolid (Spain) according to the code of ethics of the World Medical Association (Declaration of Helsinki).

Data acquisition and preprocessing were performed in an identical way as described by Nakamura *et al.*[30] In summary, the acquisition was performed using an EEG system (BrainVision, Brain Products GmbH; Munich, Germany). The electrode placement followed the 10/10 system, with 32 active electrodes. Impedances were kept below 5 kΩ. Event-related potentials (ERP) were recorded while the participants were sitting with their eyes closed. The auditory oddball task consisted of random series of 600 tones with three different kinds of tones: target (500 Hz tone), distractor (1000 Hz tone) and standard (2000 Hz tone) with probabilities of 0.20, 0.20 and 0.60, respectively. Only attended target tones (i.e., target tones followed by a mouse click from the participants) were considered. ERP signals were recorded at a sampling frequency of 500 Hz during 13 min of an auditory oddball task. After a visual inspection, signals from TP9 and TP10 electrodes were removed because of muscle artifacts. Data were re-referenced to the average activity of all active sensors obtaining 31 channels. Signals were filtered using a band-pass finite impulse response filter between 1 and 70 Hz, as well as a 50 Hz notch filter. Finally, a three-steps artifact rejection algorithm was applied to minimize ocular noise and myographic artifacts: (i) ICA was carried out and, after visual inspection, ICA components associated with artifacts were discarded; (ii) reconstruction and segmentation of the data into trials of 1 second length ranging from 300 ms before to 700 ms after stimulus onset; and (iii) automatic and adaptive trial rejection using a statistical-based thresholding method.[4]

In order to study the dynamical changes in the EEG, the single trial approach was used.[38,39] Each trials of 1 second length was divided into two time windows: baseline window ([-300 0] ms from the stimulus onset) and response window ([150 450] ms after the stimulus onset).[3,4] The baseline window is related to the resting prior to the stimulus and the response window corresponds to the cognitive response of the P300 task processing. Accordingly, the auditory oddball task is useful to analyze the dynamical neural reorganization during a cognitive processing.[3,4]

Continuous wavelet transform (*CWT*) was used in order to generate brain graphs. Wavelet transform is a useful method to accurately assess the changes of electrophysiological signals in the time-frequency plane.[40] In this study, the complex Morlet wavelet was used as 'mother' function, since it provides a plausible biological fit to EEG data.[38] It is characterized by the bandwidth (Ω_b) and the wavelet center frequency (Ω_c) parameters. They were set to 1 to obtain an adequate balance between the temporal and frequency resolution.[4] Complex Morlet can be defined as follows:

$$\varphi(t) = \frac{1}{\sqrt{\pi \cdot \Omega_b}} \cdot e^{-j\frac{2\pi \cdot \Omega_c \cdot t^2}{\Omega_b}}, \qquad (5)$$

To obtain the *CWT* coefficients, the convolution of each 1-s length EEG trial, $x(t)$, and the complex Morlet function must be calculated:

$$CWT(k,s) = \frac{1}{\sqrt{s}} \cdot \int_{-\infty}^{\infty} x(t) \cdot \varphi^*\left(\frac{t-k}{s}\right) \cdot dt, \qquad (6)$$

where s and k denote the dilation and translation factors and * represents the complex conjugation. It is important to note that edge effects are not negligible, since the trials are finite short-length time series.[38] Contrary to Fourier analysis, CWT has a variable time-frequency resolution.[36] In this regard, a Heisenberg box can be introduced. It is defined as a constant area rectangle whose height and width depends on the frequency (Δf) and the time (Δt) resolution, respectively.[36] Following previous studies, the size of the Heisenberg box was chosen to be two times Δt and Δf.[37] The influence of the edge effect changes across that representation, since Δt and Δf are not constant in the time-frequency plane. Hence, in order to overcome the errors at the beginning and the end of the wavelet power spectrum, zero padding was introduced at the extremes of each EEG trial. Nevertheless, this introduces discontinuities at the edges. Thus, the spectral content must only be considered in the time-frequency regions delimited by their respective cones of influence (COIs), where the edge effect can be ignored (see Fig. 2). In this study, target trials of 1 second length were decomposed into the baseline and response window. Therefore, it is

necessary to define one COI for each of the

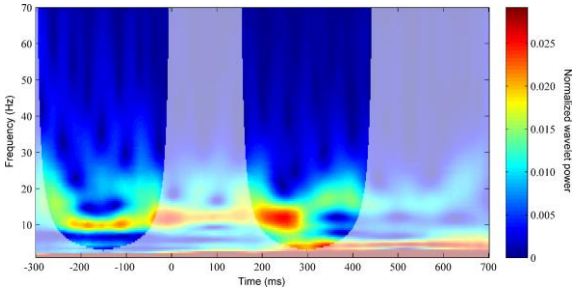

Fig. 2. Example of the normalized wavelet coefficients at Pz electrode averaged across trials in a control subject. The transparency outline represents the limits of the COI in the baseline and response windows, where the spectral content is not affected by edge effects.

aforementioned time window.

The analysis of the delta band was not performed because it could be affected by a significant bias, resulting in an inaccurate time-frequency estimation. In this regard, some studies recommend 6 cycles to accurately estimate wavelet coefficients[41]; nevertheless, two cycles can also be used at the expense of frequency resolution.[42] In this study, this latter approach was used in order to study a maximum range of the spectral content, taking care with the lower frequencies because of the possible bias introduced due to the time-frequency resolution. Thereby, the *CWT* from 4 Hz to 70 Hz was divided according to the conventional EEG frequency bands: theta (4–8 Hz), alpha (8–13 Hz), beta-1 (13–19 Hz), beta-2 (19–30 Hz) and gamma (30–70 Hz).

Graph edge weights were obtained from the *WC* without the application of any threshold to obtain the adjacency matrices. Each node of the graph corresponds to an electrode (N = 31) and each edge weight corresponds to the *WC* between the signals of the considered pair of electrodes. To obtain the *WC*, the wavelet cross-spectrum (*WCS*) between two 1-s length ERP trials was computed as follows:

$$WCS_{ij}(k,s) = CWT_i(k,s) \cdot CWT_j^*(k,s), \qquad (7)$$

where subscripts i and j identify a pair of electrodes. Once *WCS* was obtained for all pairwise electrode combinations, it was averaged across trials in two windows of interest: (i) the baseline window; and (ii) the response window. Finally, *WC* between two given electrodes i and j was calculated as follows[4,43]:

$$WC_{ij}(s) = \frac{\left|WCS_{ij}(s)\right|^2}{WCS_{ii}(s) \cdot WCS_{jj}(s)}, \qquad (8)$$

WC is a straightforward method, commonly used in previous EEG studies.[43–45] It represents the linear relationship between the amplitude of two signals in the spectral domain (nonlinear relationships are not considered).[44] *WC* was obtained for each frequency (or scale) and, then, averaged across scales in the previously defined frequency bands. Hence, one adjacency matrix was obtained for each frequency band, subject and time window (i.e., 10 adjacency matrices per subject). As a result, 790 graphs were obtained for the DATASET-real: 79 subjects × 2 time windows (baseline and response) × 5 frequency bands. Graph edge weights range from 0 to 1, since a thresholding method was not applied to the *WC* values.

4. Results

4.1. *Results on synthetic graphs*

Fig. 3 shows the changes in *SGC* and *GD* for DATASET-1 and DATASET-2 for different values of *UF*, *N* and the number of edges set to *UF* (*ES-UF*). The last parameter, *ES-UF*, reflects the balance of the edge weight distribution. When only one edge value is set to *UF* (and *UF* is large enough), the unbalance strength reaches its maximum; on the contrary, when all the edge values are set to *UF*, the edge weight distribution is completely balanced.

The first row show *SGC* values for DATASET-1 and DATASET-2. *SGC* values are exactly the same for both datasets, which implies that *SGC* is density invariant (the only difference between DATASET-1 and DATASET-2 is that graphs in DATASET-2 were normalized by their *GD*). *SGC* plots show that there is little variation in the complexity values for $N > 30$. Furthermore, there is a strong dependence between *UF* and the number of *ES-UF* needed to reach an equilibrium between a completely weight balanced distribution and a strongly weight unbalanced distribution (i.e., the maximum value of *SGC* when *N* is fixed).

On the contrary, *GD* behavior is completely different for these two datasets, since it directly depends on weight values but not on the weight distribution. The two bottom rows in Fig. 3 show the *GD* dependences for these two datasets. For DATASET-1, *GD* increases with the number of *ES-UF*. In addition, *GD* becomes higher as *UF*

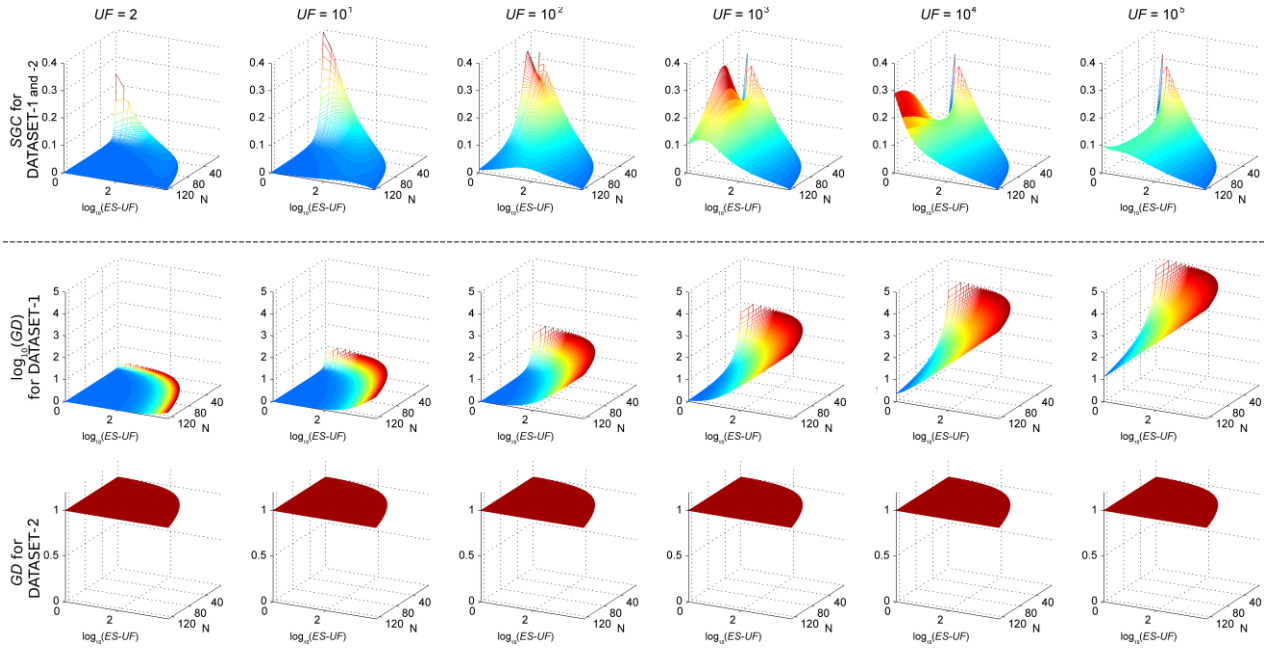

Fig. 3. *SGC* and *GD* values for DATASET-1 and DATASET-2. Note that *GD* results for DATASET-1 (second row) are represented in logarithmic scale, due to the high dependence of *GD* on *N* and *UF*.

increases (note the logarithmic scale on *z*-axis). It is important to note that all the *GD* plots of the DATASET-1 have the same shape, but it is not evident since all plots have the same scale in the axes. On the other hand, *GD* remains constant and equal to 1 for DATASET-2, since each graph was normalized by their own *GD*. Therefore, the behavior of *GD* for DATASET-1 is completely different than for DATASET-2, contrary to *SGC*. It is noteworthy that *SGC* and *GD* cannot be computed for all *N* and number of *ES-UF*, since it is impossible to generate an undirected graph of size *N* with more than $N(N-1)/2$ *ES-UF*. That is the reason why some *SGC* and *GD* values were not plotted.

The results for DATASET-3 showed that *SGC* and GD values were constant for each distribution. Therefore, *SGC* and *GD* are invariant with respect to the node degree distribution. These measures only depend on the value of the edge weights, but not on the degree of each node. Additionally, *SGC* provided complexity values of 0.026 for a uniform distribution, 0.020 for a bimodal distribution and 0.015 for a normal distribution (see Table 2). On the contrary, *GD* was not able to differentiate between these distributions.

The DATASET-4 was constructed to analyze the behavior of *SGC* for graphs with different numbers of connections. The *SGC* and *GD* results are shown in Fig. 4. Similarly to DATASET-1 and DATASET-2, *SGC* showed little variation for $N > 30$. On the other hand, *GD* showed an important dependence on the number of connections.

Table 2. *SGC* and *GD* values for all the graphs of DATASET-3. *SGC* and *GD* are independent of node degree distribution.

	Uniform distribution	Normal distribution	Bimodal distribution
GD	0.500	0.500	0.500
SGC	0.026	0.015	0.020

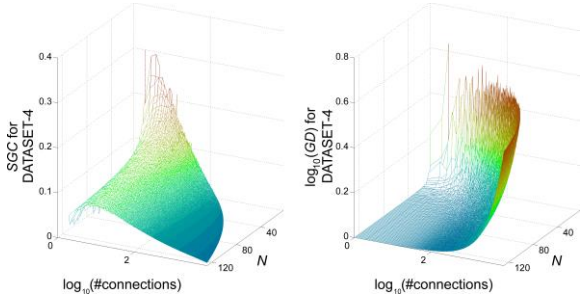

Fig. 4. *SGC* and *GD* values for DATASET-4. . Note that *GD* results are represented in logarithmic scale, due to the high dependence of *GD* on the number of connections.

Finally, Fig. 5 depicts *SGC* as a function of *H* and *UF* for *N* = 31 (number of nodes in DATASET-real). The

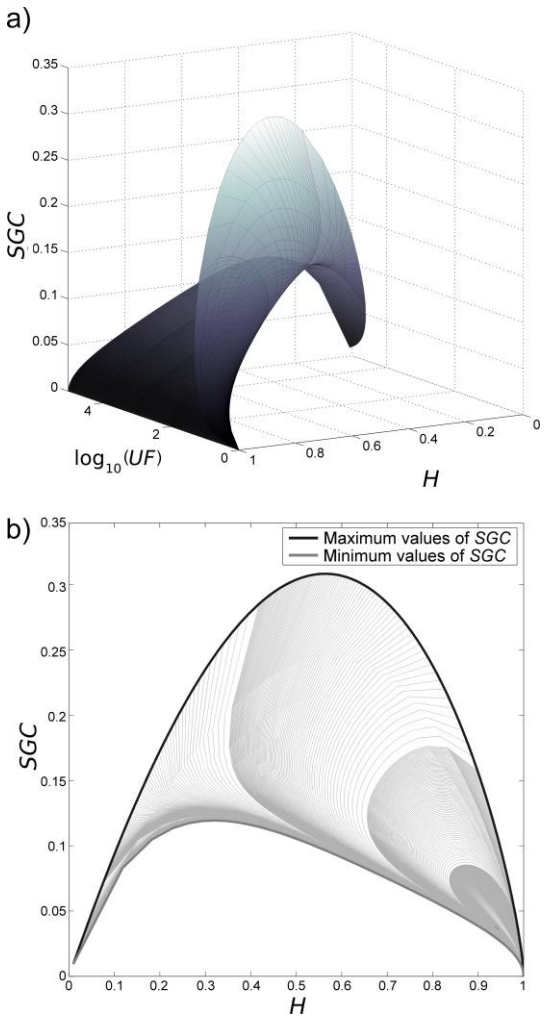

Fig. 5. a) 3D and b) 2D plots corresponding to *SGC* as function of *H* and *UF*, when *N* = 31. Maximum and minimum values of *SGC* are also depicted in b).

graphs used to generate Fig. 5 are the same as those used in DATASET-1, but with several more values of *UF* in order to obtain a compact representation of *SGC*. Fig. 5a is useful to visualize *SGC* as function of *H* and *UF*, while the maximum and minimum values of *SGC* are easily observed in the Fig. 5b.

4.2. *Results on real brain graphs: Application to schizophrenia*

We computed *SGC* for real ERP signals recorded from healthy controls and schizophrenia patients. Complexity values were compared between time windows (baseline and response) and groups (controls and patients) in the five frequency bands under study. Prior to this, an exploratory analysis was carried out to analyze data distribution. The Kolmogorov-Smirnov and the Levene tests were used to check normality and homoscedasticity of data distributions. Nonparametric tests were applied to assess statistical differences, since parametric assumptions were not met: (i) Wilcoxon signed-rank test was used to compare baseline and response network measures for within-group analyses;
and (ii) Mann-Whitney *U*-test was used for between-group analyses. In addition, Bonferroni correction for multiple comparisons was applied. Thus, the significance level was set to $\alpha = 0.01$.

Within-group analyses for *SGC* values on each group and window are shown in Fig. 6a. Only the theta band exhibited statistically differences between baseline and response windows (Z = -5.37, p = 7.83E-8, in the control group; Z = -3.05, p = 2.28E-3, in the schizophrenia group). On the other hand, *GD* was computed to validate the performance of *SGC* (Fig. 6b). Within-group analyses showed a statistically significant increase from the baseline to the response window in the theta band for both controls (Z = 5.75, p = 8.65E-9) and schizophrenia patients (Z = 3.37, p = 7.51E-4). No significant differences were found on the other frequency bands. In view of these results, only the theta band was considered for further analyses.

SGC and *GD* were baseline corrected (i.e., complexity values during baseline window were subtracted from their values during response window).[3,38] Between-group analyses showed a marked reduction on *SGC* values during the response window for both controls and schizophrenia patients. However, no significant differences were found in between-group comparisons using corrected *SGC* after Bonferroni correction though (Z = -1.95, p = 5.01E-2). Nevertheless, controls showed a more marked decrease in *SGC* values during cognitive response than patients. Regarding *GD* analysis, results indicated that controls exhibited a statistically significant more prominent increase in corrected *GD* values during the response than schizophrenia patients (Z = 2.64, p = 8.31E-3). Hence, for both network changes from baseline to response were more prominent in controls than in schizophrenia patients.

It is interesting to note that *H* increased during the response window for both controls and schizophrenia patients. This indicates that the reduction of *SGC*, which

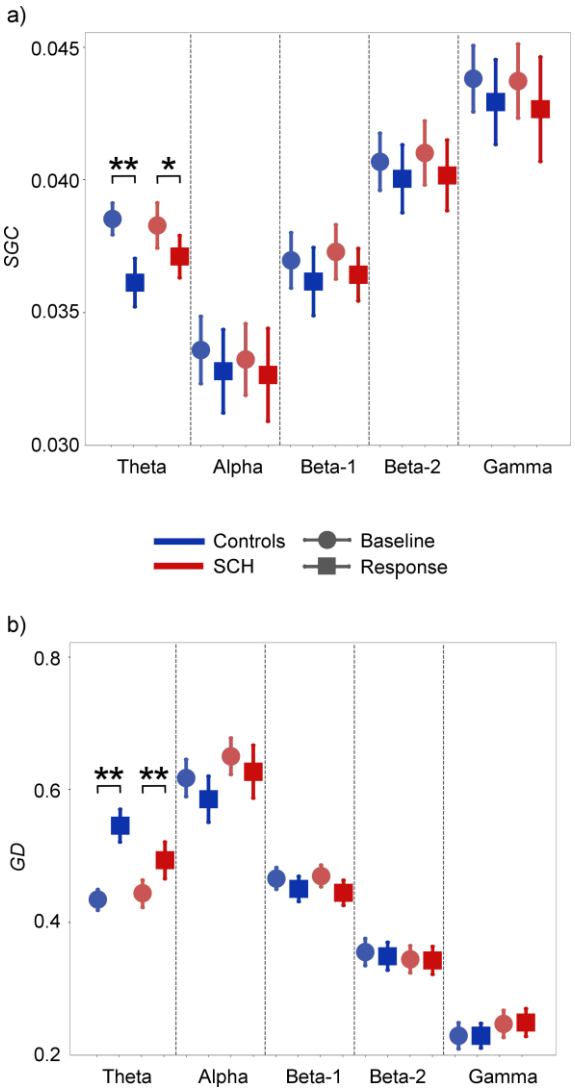

Fig. 6. a) *SGC* and b) *GD* values for each group, window and frequency band. Values are depicted as mean and standard error. * indicates $p < 0.01$, while ** indicates $p < 0.001$.

is a measure of the equilibrium between balanced and unbalanced edge eight distribution, is due to an increase in the weight balance of the network. To evaluate brain complexity dynamics during the auditory oddball task, the change of *SGC* as function of *H* from baseline to response windows for controls and schizophrenia patients is represented in Fig. 7.

5. Discussion

The main objective of this study was to propose a novel graph complexity measure and assess its behavior under different conditions using synthetic and real datasets. *SGC* is essentially normalized with respect to *GD* and independent of node degree distribution. Additionally,

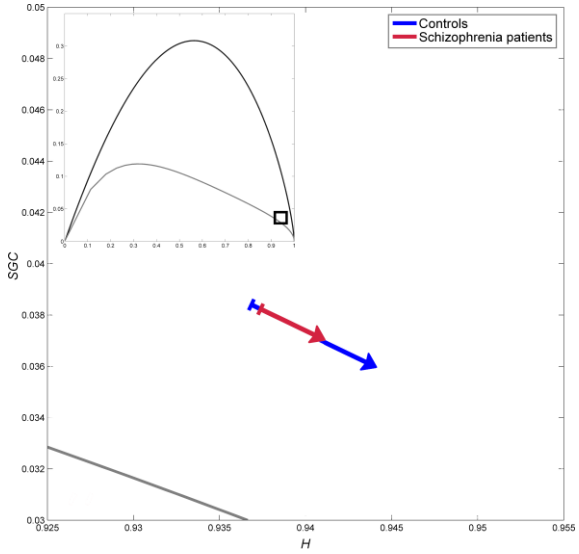

Fig. 7. Detailed plot of the complexity dynamics from baseline to response in the theta frequency band for controls (blue arrow) and schizophrenia patients (red arrow). The small figure represents the maximum and minimum possible *SGC* values for this network size. The square in the small figure corresponds to the zoomed area in the large figure. *H* increases and *SGC* decreases for both groups, but the behavior is more remarkable for controls than for schizophrenia patients.

the influence of network size on *SGC* seems to be small for $N > 30$ when *UF* takes small values. Hence, the need to make comparisons with null-hypothesis networks was not required for networks of the same size. On the other hand, statistically significant differences in network reorganization dynamics after an auditory oddball task were found between controls and schizophrenia patients with *SGC*.

5.1. *Shannon Graph Complexity dependences: Synthetic graphs*

Four synthetic datasets were generated by varying basic network characteristics, such as *N*, *UF*, *GD* and node degree distribution. DATASET-1 showed that *SGC* and *GD* depend on *N* and the number of *ES-UF*. It is important to note that a high *UF* value yields weighted graphs with similar behavior than binary graphs. Binary graphs have some connections set to 1 and others set to 0. Their behavior is similar to weighted graphs with connections set to a high *UF* value and others set to 1. Therefore, when *SGC* is applied to binary graphs, the behavior is similar to the previously showed

performance. This is a significant advantage with respect to other complexity measures, which cannot always be applied to binary and weighted graphs.[25–27] On the contrary, *SGC* can be directly applied to binary and weighted graphs.

Fig. 3 shows that the maximum of *SGC* for each *N* is always obtained for a number of *ES-UF* lower than $N(N-1)/2$. This is an important difference compared to *GD*, where the maximum is reached for *ES-UF* = $N(N-1)/2$. Therefore, *SGC* introduces a graph complexity definition more intuitive than *GD*, since graph complexity is considered as an equilibrium between 'order' and 'information' stored. If graph complexity is measured by means of *GD*,[12] a complete graph (i.e., a graph with all their nodes connected) with network connections set to the maximum value always has the highest complexity. However, this does not correspond to the intuitive notion of graph complexity, where some connections (and thus pathways) are more important than others, creating a tangled mesh of paths.[46]

DATASET-2 was assembled similarly to DATASET-1. The only difference was that the DATASET-2 graphs were normalized by their own density. That is the reason for the constant *GD* values shown in the bottom row of Fig. 3. Nevertheless, graphs with proportional weights show the same *H* and *D* values by construction; therefore, *SGC* is also the same. In this regard, the same *SGC* values were reached for DATASET-1 and DATASET-2 (see Fig. 3). This is another advantage of *SGC* in comparison with *GD*. In addition, it is not necessary to normalize the graphs by their density to compare the complexity among them, enabling the comparability between studies.

Results obtained from DATASET-3 proved that both *SGC* and *GD* are independent of node degree distribution. This implies that *SGC* is independent of network topology, which suggests that this measure provides complementary information to network measures based on topology. Two graphs with different node degree distribution or *GD*, but with the same set of weights, would have the same *SGC* value. Therefore, comparisons with null-hypothesis networks become unnecessary for networks with the same *N*. Furthermore, as we mentioned previously, the change of *SGC* is small for $N > 30$, when *UF* takes small values and *ES-UF* are fixed. Hence, the possible bias introduced when comparing with networks of different size is minimized in relation to other topology-based graph measures. DATASET-3 also provides an important difference between the two measures of graph complexity analyzed in this study. *GD* took the same value for the three different distributions. However, *SGC* results indicated that a uniform distribution of the edge weights had a higher complexity value than a normal or a bimodal distribution. This advantage of *SGC* with respect to *GD* is based on the 'order' of each distribution. A graph with maximum 'order' (a complete graph with the same value of all edges) corresponds to a delta distribution. In that case, *SGC* would provide a value equal to zero. The more the distribution under study resembles the distribution of maximum 'order', the lower the value of complexity provided by *SGC*. For that reason, the minimum complexity value was obtained with the normal distribution, with a value of 0.015 (Table 2). The bimodal distribution achieved a *SGC* value of 0.020, whereas the uniform one obtained a value of 0.026.

Regarding DATASET-4, our results showed that the *SGC* behavior with not fully connected graphs is similar to that observed for fully connected ones, since there is little variation of *SGC* for $N > 30$. On the other hand, *GD* has an important dependence on the number of connections in the graph.

Finally, it is important to note that graphs with the same size and edge values, but different topology, achieve the same value of *SGC*. Therefore, from the point of view of 'order' and amount of 'information' stored by the system, there are no differences between, for example, scale free and small-world networks (if they have the same size and edge values).

In addition, the computational cost of *SGC* is significantly lower that other complexity measures based on several iterations of mutual information[22] or on generating motifs from the original network.[26] *SGC* is based on Shannon entropy and it only needs one iteration to be computed. This is another important difference with previously proposed complexity measures.[22,26]

5.2. *Brain dynamics using Shannon Graph Complexity: Real graphs*

The results derived from DATASET-real showed that *SGC* is a metric that may allow differentiating the brain networks of controls and schizophrenia patients. For both groups, *SGC* decreased during the response window, which suggests a reduction of the equilibrium between 'order' and amount 'information' stored by the system. In addition, Fig. 6 showed higher values of *H* during the response window for both groups. Therefore, the 'order'

decreased while the amount of 'information' stored by the system increased in the subjects' brain networks during the cognitive task. However, the variation of *SGC* from the baseline to the response window is more prominent in controls, specifically in the theta band, which could evidence a deficit in the reorganization patterns in schizophrenia. In this regard, results showed that only theta band exhibited statistical differences in within-group analyses. In addition, the changes between baseline and response windows were lower in schizophrenia patients. Previous studies reported a decrease of the relative power in alpha frequency band in schizophrenia patients,[47,48] and an increase of power in theta band.[49] Furthermore, oscillations in low frequency ranges (such as theta) are related with the modulation of the long-range synchronization,[50,51] whereas high frequency ranges (such as beta and gamma) reflect synchronization in large-scale networks.[52] Thus, it can be inferred that impaired activation response of long-range interactions might contribute to the pathological process of schizophrenia, which usually shows an integration deficit among distant brain areas.[29] In view of these results, the present study reports similar ideas to previous ones, which suggested that schizophrenia is accompanied by a disrupted network reorganization of neural functions, mainly in long-range interactions.[3,53,54]

Our results also agree with previous studies that linked impaired network reorganization capacity with the aberrant salience and the disconnection hypotheses.[55,56] In this regard, Bachiller *et al.*[4] posed the idea that schizophrenia patients failed to change their coupling dynamics between stimulus response and baseline when performing a stimulus processing. It can be related to a diminished ability to optimize the neural synchronicity leading to a functional disconnection. This idea was clearly shown by *GD* results. Controls showed a significant increase in *GD* during the response, which implies a global increment of connectivity patterns. As reported in task-related studies,[4,57] an increase of ERP synchronicity on the theta frequency band is observed during cognitive processing. Nonetheless, schizophrenia patients usually show a failure to modulate synchronous activity, particularly when asked to attend to target stimuli.[4,58] This modulation deficit produces lower *WC* values for schizophrenia patients than for controls. Therefore, it seems reasonable that schizophrenia patients exhibited lower *GD* values during the response window.

There are important aspects that indicate the complementarity of *SGC* and *GD*. On the one hand, *SGC* (jointly with *H*) showed that the weight distribution is more balanced during the response compared to baseline (see Fig. 6). Taking into account only *SGC* results, the increased balance could be a consequence of: (i) a prominent increase in the value of weak connections (i.e., secondary neural pathways); (ii) a decrease in the value of the connections with higher values; or (iii) the combined effect of the previous two points. On the other hand, *GD* showed an increase, on average, of the edge weights during the response window. Therefore, the increase of edge values for the secondary neural pathways should have a higher effect than a possible decrease in the connections with higher values (option (i)). Furthermore, *SGC* modulation is higher for controls, but statistically significant differences were not found between the baseline windows of both groups. Thus, it is likely that secondary neural pathways can be strengthened in controls compared to schizophrenia patients during cognitive processing. This strengthening balances the weight distribution, which could increase the reliability and the information propagation speed in the brain. Therefore, controls can reorganize their brain network between different areas in a flexible and transient way in order to coordinate the response to the cognitive task. The previous inferences have only been possible due to the complementary information provided by *SGC* and *GD*. Although the statistical differences between healthy subjects and schizophrenia patients are more marked for *GD* than for *SGC*, it is important to note that the second objective of this study is to assess the usefulness of *SGC* in determining the properties of the real brain networks. In this regard, *SGC* provided different and complementary information to that of a classical measure of graph complexity, *GD*, meeting the second objective of the study.

The idea of classifying brain graph connections in different topological levels (primary and secondary connections) is in line with a recent concept introduced in neuroscience to model the brain network: the minimum spanning tree (MST).[46,59] MST is an acyclic subgraph that connects all nodes using exactly $N-1$ edges while minimizing distance between nodes (i.e., maximizing the connection strength).[60] It represents a critical backbone of information flow in weighted networks, providing information about how the brain structures the information in different topological levels.

The nodes involved could be similar to those forming the weighted "rich club" (i.e., a subset of high-degree nodes that are connected by a larger fraction of the most highly weighted edges in the graph that expected by chance).[61] Thus, the brain network is modeled as a two topological levels structure. The first topological level is formed by the main connections (i.e., the MST backbone and the "rich club" motifs). The second topological level is formed by secondary neural pathways, which are removed in the MST model. Thus, this idea supports our concept of network complexity: the brain is a network halfway between a completely balanced and unbalanced weight distribution, where the higher-level topologies are part of the previously mentioned MST backbone. *SGC* is useful to evaluate the relationship between primary and secondary pathways in terms of weight balance, which can support the existence of "rich club" assemblies in the brain network. In this regard, it is commonly accepted that the archetypal brain network is sparsely connected between nodes in different modules.[62] In this study, *SGC* showed that weak connections increase their strength during the response window, generating new alternative pathways that should work to increment network integration. It is noteworthy that several EEG studies reported an increase in brain network integration during cognitive processing.[63,64] This integration, usually measured by means of the path length, is reduced in schizophrenia patients compared to controls during an oddball task,[5] which is again in agreement with the disconnection hypothesis.[29] The present results support an altered information processing in schizophrenia, which may not characterize, however, all the patients in this syndrome, given its likely heterogeneous biological substrate.[65]

5.3. *Limitations and future lines of research*

Some methodological issues of this study merit consideration. Firstly, *SGC* does not provide information about graph topology. Although this is an important advantage because the requirement for a surrogate process is avoided by comparing networks with the same *N*, the lack of this information requires the use of complementary measures in order to obtain a global vision of the network. Nonetheless, the need for various measures to fully characterize a graph is commonly accepted.[66,67] Individually, topological features do not provide information on the connectivity balance or the strength of the functional neural connections. In our opinion, this edge weight distribution balance has a very important role in the analysis of the impact of network complexity. Therefore, the lack of this information could lead to ignoring important aspects of the brain network.

The second methodological issue is related to the intrinsic *SGC* property as an entropy-based measure. Previous studies suggested that entropy quantifiers might overestimate the irregularity in the brain network.[68] This could explain why entropy values obtained from brain networks reached values close to 1, as shown in Fig. 7. Different entropy measures could provide different degrees of disorder estimation. Future works should address this concern by quantifying the irregularity by means of other entropy measures. Likewise, different disequilibrium measures based on more complex measures of distance (Euclidean distance was used in this study) could provide complementary results.

Thirdly, the methods used to estimate the connectivity between brain areas could have a high impact on measures that are strongly dependent on edge weights. DATASET-real was obtained by applying *WC* to EEG recordings. The choice of this connectivity measure was motivated by its widespread use as a method for weight estimation in functional brain graphs.[44] Coherence is a straightforward method that assesses the linear relation between the amplitude of two signals in the frequency domain. However, it is sensitive to volume conduction,[44] which could lead to an erroneously high estimation of connectivity between two network nodes.[44,69] In this regard, a statistical threshold to remove spurious connections could help to clarify the results. Future works should be carried out to evaluate *SGC* behavior in graphs obtained using metrics that do not overestimate the connectivity between nodes, such as phase-based measures. In addition, it could be interesting to apply multivariate approaches for causal interactions between nodes, since directed edges can be interpreted in a more physiological way. The application of *SGC* in these conditions would not need any reformulation, since it is applicable to directed graphs. Nonetheless, it is important to note that the proposed measure is an extension of a metric originated in information theory by considering normalized weights as probabilities. For that reason, it is not possible to compute *SGC* when a graph takes negative edge weights. In this regard, an interesting future line of research could be a more theoretical approach of the interpretation of the proposed metric. It would provide more meaningful and general results.

6. Conclusions

Several pieces of evidence suggest that the edge weight distribution of complex brain networks is directly related to reliability aspects and to its information propagation speed. Therefore, graph measures that evaluate the weight distribution are fully justified. *SGC* was introduced as a useful alternative to *GD* and other graph complexity measures. In this study, we proved the independence of *SGC* with respect to basic graph characteristics, in addition to an almost small dependence on *N* when *UF* takes small values.

Our results from real brain graphs indicate that *SGC* is particularly useful to determine the intrinsic properties of neural dynamics during a cognitive task. Specifically, *SGC* results suggest that the auditory oddball task elicits an increment of the connection weights, mainly in the edges related to secondary neural links. This provides alternative pathways to the neural backbone. Another important remark is the prominent change in *SGC* and *GD* observed in controls compared to schizophrenia patients. These insights are in line with the disconnection and aberrant salience hypotheses. They involve a deficit in neural network reorganization during cognitive processing that could lead to a lower functional integration of the brain network.

Acknowledgements

This research project was supported in part by: the "Ministerio de Economía y Competitividad" and FEDER under project TEC2014-53196-R; the "Fondo de Investigaciones Sanitarias (Instituto de Salud Carlos III)" under projects FIS PI11/02203 and PI15/00299; and the "Gerencia Regional de Salud de Castilla y León" under projects GRS 932/A/14 and GRS 1134/A/15. A. Bachiller and J. Gomez-Pilar were in receipt of a PIF-UVA grant from University of Valladolid. A. Lubeiro has a predoctoral scholarship from the "Junta de Castilla y León" and European Social Fund. P. Núñez was in receipt of a 'Promoción de empleo joven e implantación de la Garantía Juvenil en I+D+i' grant from 'Ministerio de Economía y Competitividad' and the University of Valladolid. We would like to express our gratitude to the Psychiatry Service of the Clinical University Hospital of Valladolid (Spain), for their help and support.

References

1. Stam, C. J. et al. Graph theoretical analysis of magnetoencephalographic functional connectivity in Alzheimer's disease. *Brain* **132**, 213–224 (2009).
2. Bassett, D. S., Nelson, B. G., Mueller, B. A., Camchong, J. & Lim, K. O. Altered resting state complexity in schizophrenia. *Neuroimage* **59**, 2196–2207 (2012).
3. Gomez-Pilar, J. et al. Neural network reorganization analysis during an auditory oddball task in schizophrenia using wavelet entropy. *Entropy* **17**, 5241–5256 (2015).
4. Bachiller, A. et al. A comparative study of event-related coupling patterns during an auditory oddball task in schizophrenia. *J. Neural Eng*. **12**, 16007 (2015).
5. Shim, M., Kim, D. W., Lee, S. H. & Im, C. H. Disruptions in small-world cortical functional connectivity network during an auditory oddball paradigm task in patients with schizophrenia. *Schizophr. Res*. **156**, 197–203 (2014).
6. Deco, G., Tononi, G., Boly, M. & Kringelbach, M. L. Rethinking segregation and integration: contributions of whole-brain modelling. *Nat. Rev. Neurosci.* **16**, 430–439 (2015).
7. Boccaletti, S., Latora, V., Moreno, Y., Chavez, M. & Hwang, D. U. Complex networks: Structure and dynamics. *Phys. Rep.* **424**, 175–308 (2006).
8. Bullmore, E. T. & Bassett, D. S. Brain graphs: graphical models of the human brain connectome. *Annu. Rev. Clin. Psychol.* **7**, 113–140 (2011).
9. Ansmann, G. & Lehnertz, K. Surrogate-assisted analysis of weighted functional brain networks. *J. Neurosci. Methods* **208**, 165–172 (2012).
10. Costa, L. D. F., Rodrigues, F. A., Travieso, G. & Boas, P. R. V. Characterization of complex networks: A survey of measurements. *Adv. Phys*. **56**, 167–242 (2005).
11. Rubinov, M. & Sporns, O. Complex network measures of brain connectivity: Uses and interpretations. *Neuroimage* **52**, 1059–1069 (2010).
12. Bonchev, D. & Buck, G. A. in Complexity in Chemistry, Biology, and Ecology (ed. Media, S. S. & B.) 191–235 (In Complexity in Chemistry, Biology, and Ecology. Springer US, 2007). doi:10.1007/0-387-25871-X
13. Watts, D. & Strogatz, S. Collective dynamics of small-world networks. *Nature* **393**, 440–442 (1998).
14. Astolfi, L. et al. Assessing cortical functional connectivity by linear inverse estimation and directed transfer function: Simulations and application to real data. *Clin. Neurophysiol.* **116**, 920–932 (2005).
15. Fallani, F. D. V. et al. Extracting Information from Cortical Connectivity Patterns Estimated from High Resolution EEG Recordings : A Theoretical Graph Approach. *Brain Topogr.* **19**, 125–136 (2007).
16. Ahmadlou, M., Adeli, H. & Adeli, A. Graph theoretical analysis of organization of functional brain networks in ADHD. *Clin. EEG Neurosci.* **43**, 5–13 (2012).

17. Sporns, O. & Zwi, J. D. The small world of the cerebral cortex. *Neuroinformatics* **2**, 145–162 (2004).
18. Chiappalone, M., Vato, A., Berdondini, L., Koudelka-Hep, M. & Martinoia, S. Network dynamics and synchronous activity in cultured cortical neurons. *Int. J. Neural Syst.* **17**, 87–103 (2007).
19. Han, F., Wiercigroch, M., Fang, J.-A. & Wang, Z. Excitement and synchronization of small-world neuronal networks with short-term synaptic plasticity. *Int. J. Neural Syst.* **21**, 415–425 (2011).
20. Neefs, P. J., Steur, E. & Nijmeijer, H. Network complexity and synchronous behavior - an experimental approach. *Int. J. Neural Syst.* **20**, 233–247 (2010).
21. Yamanishi, T., Liu, J.-Q. & Nishimura, H. Modeling fluctuations in default-mode brain network using a spiking neural network. *Int. J. Neural Syst.* **22**, 1250016 (2012).
22. Tononi, G., Edelman, G. M. & Sporns, O. Complexity and coherency : integrating information in the brain. *Trends Cogn. Sci.* **2**, 474–484 (1998).
23. Ahmadlou, M., Adeli, H. & Adeli, A. New diagnostic EEG markers of the Alzheimer's disease using visibility graph. *J. Neural Transm.* **117**, 1099–1109 (2010).
24. Ahmadlou, M. & Adeli, H. Visibility graph similarity: A new measure of generalized synchronization in coupled dynamic systems. *Phys. D Nonlinear Phenom.* **241**, 326–332 (2012).
25. Machta, B. & Machta, J. Parallel dynamics and computational complexity of network growth models. Phys. Rev. E - Stat. Nonlinear, *Soft Matter Phys.* **71**, 1–9 (2005).
26. Meyer-Ortmanns, H. Functional complexity measure for networks. *Physica A* **337**, 679–690 (2004).
27. Claussen, J. C. Offdiagonal complexity: A computationally quick complexity measure for graphs and networks. *Physica A* **375**, 365–373 (2007).
28. Morabito, F. C. et al. A longitudinal EEG study of Alzheimer's disease progression based on a complex network approach. *Int. J. Neural Syst.* **25**, 1550005 (2015).
29. Friston, K. J. The disconnection hypothesis. *Schizophr. Res.* **30**, 115–125 (1998).
30. Nakamura, T., Hillary, F. G. & Biswal, B. B. Resting network plasticity following brain injury. *PLoS One* **4**, e8220 (2009).
31. van Wijk, B. C. M., Stam, C. J. & Daffertshofer, A. Comparing brain networks of different size and connectivity density using graph theory. *PLoS One* **5**, e13701 (2010).
32. Gomez-Pilar, J. et al. Novel measure of the weigh distribution balance on the brain network: graph complexity applied to schizophrenia. *Proceedings of the 35th Annual International Conference of the IEEE Engineering in Medicine and Biology Society Conference* 700–703 (2016).
33. Shannon, C. E. A mathematical theory of communication. Bell Syst. Tech. J. **27**, 379–423 (1948).
34. Martin, M. T., Plastino, A. & Rosso, O. A. Statistical complexity and disequilibrium. *Phys. Lett. A* **311**, 126–132 (2003).
35. López-Ruiz, R., Mancini, H. L. & Calbet, X. A Statistical Measure of Complexity. *Phys. Lett. A* **209**, (2002).
36. American Psychiatric Association. Diagnostic and Statistical Manual of Mental Disorders, 5th Edition: DSM-5. (Arlington: American Psychiatric Publishing, 2013). doi:10.1176/appi.books.9780890425596.893619
37. Kay, S. R., Opler, L. A. & Lindenmayer, J. P. The Positive and Negative Syndrome Scale (PANSS): Rationale and standardisation. *Br. J. Psychiatry* **155**, 59–65 (1989).
38. Roach, B. J. & Mathalon, D. H. Event-related EEG time-frequency analysis: An overview of measures and an analysis of early gamma band phase locking in schizophrenia. *Schizophr. Bull.* **34**, 907–926 (2008).
39. Michalopoulos, K., Zervakis, M., Deiber, M.-P. & Bourbakis, N. Classification of EEG single trial microstates using local global graphs and discrete hidden Markov models. *Int. J. Neural Syst.* **26**, 1650036 (2016).
40. Mallat, S. in A Wavelet Tour of Signal Processing 20–41 (1999). doi:10.1016/B978-012466606-1/50004-0
41. Herrmann, C. S., Grigutsch, M. & Busch, N. a. EEG oscillations and wavelet analysis. *Eventrelated potentials A methods Handb*. 1–39 (1999).
42. Tallon-Baudry, C., Bertrand, O., Delpuech, C. & Permier, J. Oscillatory gamma-band (30-70 Hz) activity induced by a visual search task in humans. *J. Neurosci.* **17**, 722–734 (1997).
43. Sankari, Z., Adeli, H. & Adeli, A. Wavelet Coherence Model for Diagnosis of Alzheimer Disease. *Clin. EEG Neurosc.* **43**, 268–278 (2016).
44. van Diessen, E. et al. Opportunities and methodological challenges in EEG and MEG resting state functional brain network research. *Clin. Neurophysiol.* **126**, 1468–1481 (2015).
45. Sankari, Z. & Adeli, H. Probabilistic neural networks for diagnosis of Alzheimer ' s disease using conventional and wavelet coherence. *J. Neurosci. Methods* **197**, 165–170 (2011).
46. Tewarie, P., van Dellen, E., Hillebrand, A. & Stam, C. J. The minimum spanning tree: An unbiased method for brain network analysis. *Neuroimage* **104**, 177–188 (2015).
47. Ford, J. M., Roach, B. J., Faustman, W. O. & Mathalon, D. H. Synch before you speak: Auditory hallucinations in schizophrenia. *Am. J. Psychiatry* **164**, 458–466 (2007).
48. Bramon, E., Rabe-Hesketh, S., Sham, P., Murray, R. M. & Frangou, S. Meta-analysis of the P300 and P50 waveforms in schizophrenia. *Schizophr. Res.* **70**, 315–329 (2004).
49. Polich, J. Updating P300: An integrative theory of P3a and P3b. *Clin. Neurophysiol.* **118**, 2128–2148 (2007).
50. Sauseng, P. et al. Theta coupling in the human electroencephalogram during a working memory task. *Neurosci. Lett.* **354**, 123–126 (2004).
51. von Stein, A., Chiang, C. & König, P. Top-down processing mediated by interareal synchronization. *Proc. Natl. Acad. Sci. U. S. A.* **97**, 14748–14753 (2000).

52. Uhlhaas, P. J. Dysconnectivity, large-scale networks and neuronal dynamics in schizophrenia. *Curr. Opin. Neurobiol.* **23**, 283–290 (2013).
53. Gomez-Pilar, J. et al. Association between electroencephalographic modulation, psychotic-like experiences and cognitive performance in the general population. *Psychiatry Clin. Neurosci.* **70**, 286–294 (2016).
54. Schmiedt, C., Brand, a., Hildebrandt, H. & Basar-Eroglu, C. Event-related theta oscillations during working memory tasks in patients with schizophrenia and healthy controls. *Cogn. Brain Res.* **25**, 936–947 (2005).
55. Kapur, S. Psychosis as a state of aberrant salience: A framework linking biology, phenomenology, and pharmacology in schizophrenia. *Am. J. Psychiatry* **160**, 13–23 (2003).
56. Stephan, K. E., Friston, K. J. & Frith, C. D. Dysconnection in Schizophrenia: From abnormal synaptic plasticity to failures of self-monitoring. *Schizophr. Bull.* **35**, 509–527 (2009).
57. Uhlhaas, P. J. & Singer, W. Abnormal neural oscillations and synchrony in schizophrenia. *Nat. Rev. Neurosci.* **11**, 100–113 (2010).
58. Uhlhaas, P. J., Haenschel, C., Nikolić, D. & Singer, W. The role of oscillations and synchrony in cortical networks and their putative relevance for the pathophysiology of schizophrenia. *Schizophr. Bull.* **34**, 927–943 (2008).
59. Ortega, G. J., Sola, R. G. & Pastor, J. Complex network analysis of human ECoG data. *Neurosci. Lett.* **447**, 129–133 (2008).
60. Prim, R. C. Shortest connection networks and some generalizations. *Bell Syst. Tech. J.* **36**, 1389–1401 (1957).
61. Fortino, A., Zalesky, A. & Bullmore, E. Fundamentals of brain network analysis. (Academic Press, 2016).
62. Bullmore, E. & Sporns, O. Complex brain networks: graph theoretical analysis of structural and functional systems. *Nat. Rev. Neurosci.* **10**, 186–198 (2009).
63. Rubinov, M. et al. Small-world properties of nonlinear brain activity in schizophrenia. *Hum. Brain Mapp.* **30**, 403–416 (2009).
64. Pachou, E. et al. Working memory in schizophrenia: An EEG study using power spectrum and coherence analysis to estimate cortical activation and network behavior. *Brain Topogr.* **21**, 128–137 (2008).
65. Molina, V. & Blanco, J. A. A proposal for reframing schizophrenia research. 201, 744–752 (2013).
66. Bassett, D. S. & Bullmore, E. Small-world brain networks. *Neuroscientist* **12**, 512–523 (2006).
67. Rubinov, M. et al. Small-world properties of nonlinear brain activity in schizophrenia. *Hum. Brain Mapp.* **30**, 403–416 (2009).
68. Bruña, R. et al. Analysis of spontaneous MEG activity in mild cognitive impairment and Alzheimer's disease using spectral entropies and statistical complexity measures. *J. Neural Eng.* **9**, 36007 (2012).
69. Nunez, P. L. et al. EEG coherency I: Statistics, reference electrode, volume conduction, Laplacians, cortical imaging, and interpretation at multiple scales. *Electroencephalogr. Clin. Neurophysiol.* **103**, 499–515 (1997).